

The Coefficient η_3 of the $|\Delta S|=2$ -Hamiltonian in the Next-To-Leading Order

Stefan Herrlich ^{a *}

^aDESY-IFH, Platanenallee 6, D-15738 Zeuthen, Germany

I present the calculation of the QCD short distance coefficient η_3 of the $|\Delta S|=2$ -hamiltonian in the next-to-leading order (NLO) of renormalization group improved perturbation theory. It involves the two-loop mixing of bilocal structures composed of two $|\Delta S|=1$ operators into $|\Delta S|=2$ operators. The next-to-leading order corrections enhance η_3 by 27% to

$$\eta_3 = 0.47_{-0.04}^{+0.03}$$

thereby affecting the phenomenology of the CP-parameter ϵ_K sizeably. η_3 depends on the physical input parameters m_t , m_c and $\Lambda_{\overline{\text{MS}}}$ only weakly. The quoted error stems from factorization scale dependences, which have reduced compared to the old leading log result. We further discuss some field theoretical aspects of the calculation such as the renormalization group equation for Green's functions with two operator insertions and the renormalization scheme dependence caused by the presence of evanescent operators. This article is based on work done in collaboration with U. Nierste.

1. Introduction

The effective low-energy hamiltonian inducing the $|\Delta S|=2$ -transition reads:

$$\begin{aligned} H^{|\Delta S|=2} &= \lambda_c^2 H^c + \lambda_t^2 H^t + 2\lambda_c \lambda_t H^{ct} \\ &= \frac{G_F^2}{16\pi^2} M_W^2 \left[\lambda_c^2 \eta_1^* S(x_c^*) + \lambda_t^2 \eta_2^* S(x_t^*) \right. \\ &\quad \left. + 2\lambda_c \lambda_t \eta_3^* S(x_c^*, x_t^*) \right] b(\mu) \tilde{Q}_{S2}(\mu) \\ &\quad + \text{h.c.} \end{aligned} \quad (1)$$

Here G_F denotes Fermi's constant, M_W is the W boson mass, $\lambda_j = V_{jd} V_{js}^*$, $j = c, t$ comprises the CKM-factors, and \tilde{Q}_{S2} is the local dimension-six $|\Delta S|=2$ four-quark operator

$$\tilde{Q}_{S2} = [\bar{s}\gamma_\mu (1 - \gamma_5) d] \cdot [\bar{s}\gamma_\mu (1 - \gamma_5) d] \quad (2)$$

The $x_q^* = m_q^{*2}/M_W^2$, $q = c, t$ encode the running quark masses $m_q^* = m_q(m_q)$ in the $\overline{\text{MS}}$ scheme. In writing (1) the GIM mechanism $\lambda_u + \lambda_c + \lambda_t = 0$ has been used to eliminate λ_u . Further we have set

*e-mail: herrl@feynman.t30.physik.tu-muenchen.de

$m_u = 0$. The Inami-Lim functions $S(x)$, $S(x, y)$ describe the $|\Delta S|=2$ -transition amplitude in the absence of QCD. They read:

$$S(x_t) = x_t \left[\frac{1}{4} + \frac{9}{4} \frac{1}{1-x_t} - \frac{3}{2} \frac{1}{(1-x_t)^2} \right] - \frac{3}{2} \left[\frac{x_t}{1-x_t} \right]^3 \ln x_t, \quad (3a)$$

$$S(x_c) = x_c + O(x_c^2), \quad (3b)$$

$$S(x_c, x_t) = -x_c \ln x_c + x_c F(x_t) + O(x_c^2 \ln x_c), \quad (3c)$$

with

$$F(x_t) = \frac{x_t^2 - 8x_t + 4}{4(1-x_t)^2} \ln x_t + \frac{3}{4} \frac{x_t}{x_t - 1}. \quad (4)$$

In (3b) and (3c) we have only kept terms which are larger than those of order $(m_s m_c)/M_W^2$ neglected by setting the external momenta to zero.

In (1) the short-distance QCD corrections are comprised in the coefficients η_1^* , η_2^* and η_3^* with their explicit dependence on the renormalization scale μ factored out in the function $b(\mu)$. In absence of QCD corrections $\eta_i^* b(\mu) = 1$.

Table 1 summarizes the logarithms summed by the forthcoming renormalization group (RG) evolution from M_W down to m_c in the different orders.

Table 1

Logarithms summed by the RG evolution from M_W down to m_c for the three terms in (1), $n = 0, 1, 2, \dots$. The last line shows the order in which the dependence on m_t enters.

Order	H^c	H^t	H^{ct}
LO	$(\alpha_s \ln x_c)^n$	$(\alpha_s \ln x_c)^n$	$(\alpha_s \ln x_c)^n \ln x_c$
NLO	$\alpha_s (\alpha_s \ln x_c)^n$	$\alpha_s (\alpha_s \ln x_c)^n$	$(\alpha_s \ln x_c)^n$
m_t	none	in LO	in NLO

The first complete determination of the coefficients η_i , $i = 1, 2, 3$ in the leading order (LO) is due to Gilman and Wise [1]. However, the LO expressions have several conceptual drawbacks:

- i) The fundamental QCD scale parameter $\Lambda_{\overline{\text{MS}}}$ is not well-defined in the LO.
- ii) The quark mass dependence of the η_i 's is not correctly reproduced by the LO expressions. Especially the m_t^* -dependent terms in $\eta_3^* \cdot S(x_c^*, x_t^*)$ already belong to the NLO.
- iii) Similarly the question of the *definition* of the quark masses (i.e. the renormalization scheme and scale) to be used in (1) is a next-to-leading order issue.
- iv) The LO results for η_1 and η_3 show a large dependence on the factorization scales, at which one integrates out heavy particles. In the NLO these uncertainties are reduced considerably.
- v) One must go to the NLO to judge whether perturbation theory works, i.e. whether the radiative corrections are small. After all the corrections can be sizeable.

To overcome the limitations listed above one has to go to the next-to-leading order (NLO). This programme has been started with the calculation of η_2^* by Buras, Jamin and Weisz [2]. Then Nierste and I have derived the NLO expressions for η_1^* [3]

and η_3^* [4]. This article will essentially deal with the term H^{ct} of (1) and is based on [4].

2. The NLO calculation of η_3 above the charm threshold

Here we will shortly describe how the large logarithm $\ln x_c$ present in (3c) is summed to all orders in perturbation theory. This is done in two steps: First one sets up an effective lagrangian $\mathcal{L}_{\text{eff}}^{|\Delta S|=2}$ in which the W boson and the top quark are removed as dynamic degrees of freedom. In $\mathcal{L}_{\text{eff}}^{|\Delta S|=2}$ the $|\Delta S|=1$ and $|\Delta S|=2$ transitions are described by local four-quark operators, which are multiplied by Wilson coefficients. The general structure of $\mathcal{L}_{\text{eff}}^{|\Delta S|=2}$ reads:

$$\mathcal{L}_{\text{eff}}^{|\Delta S|=2} = -\frac{G_F}{\sqrt{2}} V_{\text{CKM}} \sum_k C_k Q_k - \frac{G_F^2}{2} V_{\text{CKM}} \sum_l \tilde{C}_l \tilde{Q}_l. \quad (5)$$

Here the V_{CKM} denote products of CKM elements. The Q_k , \tilde{Q}_l represent local $|\Delta S|=1$ and $|\Delta S|=2$ operators and the C_k , \tilde{C}_l are the corresponding Wilson coefficient functions. The $|\Delta S|=1$ part of (5) contributes to $|\Delta S|=2$ transitions via diagrams of the type displayed in Fig. 1. The Wil-

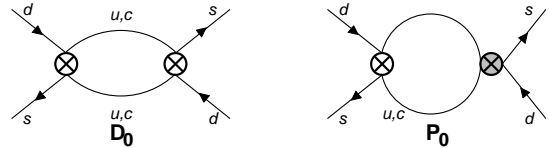


Figure 1. *The diagrams D_0 and P_0 in the effective five- and four-quark theory. The light crosses denote insertions of local $|\Delta S|=1$ current-current operators, the grey ones insertion of local $|\Delta S|=1$ four-quark penguin operators.*

son coefficients are fixed at a factorization scale $\mu_{tW} = O(M_W, m_t)$ by the requirement that the $|\Delta S|=1$ and $|\Delta S|=2$ Green's functions derived from (5) are equal to the same quantities calculated with the full SM lagrangian. The effect of this procedure is that the $\ln x_c$ present

in (3c) is split as $\ln(\mu_{tW}/M_W) + \ln(m_c/\mu_{tW})$. Here the former term resides in the Wilson coefficients while the latter is contained in the matrix elements of the local operators. The choice $\mu_{tW} = O(M_W, m_t)$ ensures that the Wilson coefficients do not contain large logarithms and therefore can be reliably calculated in ordinary perturbation theory.

The second step is the RG evolution of the Wilson coefficients from the scale μ_{tW} down to $\mu_c = O(m_c)$ which sums $\ln(\mu_c/\mu_{tW})$.¹⁾

2.1. The Operator Basis

Let us now construct $\mathcal{L}_{\text{eff}}^{|\Delta S|=2}$ in (5) as far it is needed for the calculation of η_3 . Since the presence of $|\Delta S|=2$ terms in (5) does not affect the $|\Delta S|=1$ part of $\mathcal{L}_{\text{eff}}^{|\Delta S|=2}$, we can simply take the latter from [5–7]. They consist of the following set of operators:

$$Q_1^{kl} = (\bar{s}\gamma_\mu Lk) \cdot (\bar{l}\gamma^\mu Ld) \cdot \tilde{\mathbf{1}}, \quad (6a)$$

$$Q_2^{kl} = (\bar{s}\gamma_\mu Lk) \cdot (\bar{l}\gamma^\mu Ld) \cdot \mathbf{1}, \quad (6b)$$

$$Q_3 = (\bar{s}\gamma_\mu Ld) \cdot \sum_{q=d,u,s,\dots} (\bar{q}\gamma^\mu Lq) \cdot \mathbf{1}, \quad (6c)$$

$$Q_4 = (\bar{s}\gamma_\mu Ld) \cdot \sum_{q=d,u,s,\dots} (\bar{q}\gamma^\mu Lq) \cdot \tilde{\mathbf{1}}, \quad (6d)$$

$$Q_5 = (\bar{s}\gamma_\mu Ld) \cdot \sum_{q=d,u,s,\dots} (\bar{q}\gamma^\mu Rq) \cdot \mathbf{1}, \quad (6e)$$

$$Q_6 = (\bar{s}\gamma_\mu Ld) \cdot \sum_{q=d,u,s,\dots} (\bar{q}\gamma^\mu Rq) \cdot \tilde{\mathbf{1}}. \quad (6f)$$

Here the Q_i^{kl} , $i = 1, 2$, $k, l = u, c$ represent the $|\Delta S|=1$ current-current operators, the Q_i , $i = 3, \dots, 6$ the QCD-penguin operators. The sum in (6c)–(6f) runs over all active flavours. Further $L, R = (1 \mp \gamma_5)$ and $\mathbf{1}, \tilde{\mathbf{1}}$ denote color singlet and anti-singlet, i.e. $Q_1^{kl} = (\bar{s}_i \gamma_\mu L k_j) \cdot (\bar{l}_j \gamma^\mu L d_i)$ with i, j being color indices.

Further we need the $|\Delta S|=2$ operators present in (5). Consider first the diagram D_0 of Fig. 1 with two internal charm quarks and zero external momenta. The only physical dimension-eight $|\Delta S|=2$ operator required to absorb its divergence

¹⁾For simplicity we ignore the intermediate scale $\mu_b = O(m_b)$ at which the bottom quark gets integrated out.

reads

$$\tilde{Q}_7 = \frac{m_c^2}{g^2 \mu^{2\varepsilon}} \tilde{Q}_{S2} = \frac{m_c^2}{g^2 \mu^{2\varepsilon}} \cdot \bar{s}\gamma_\mu Ld \cdot \bar{s}\gamma^\mu Ld, \quad (7)$$

which follows from power counting and the absence of any non-zero mass parameter apart from m_c . The inverse powers of g are introduced for later convenience as in [1]. One may arbitrarily shift such factors from the Wilson coefficient into the definition of the operator. The factor $\mu^{-2\varepsilon}$ stems from $g_{\text{bare}} = Z_g g \mu^\varepsilon$ and the fact that

$$\tilde{Q}_7^{\text{bare}} = \frac{m_{c,\text{bare}}^2}{g_{\text{bare}}^2} [\bar{s}\gamma_\mu Ld \cdot \bar{s}\gamma^\mu Ld]^{\text{bare}}. \quad (8)$$

must be independent of μ .²⁾ Any other dimension-eight $|\Delta S|=2$ operator contains one or two powers of m_c less than \tilde{Q}_7 and derivatives and/or gluon fields instead. Their on-shell matrix elements are suppressed by powers of m_s/m_c with respect to those of \tilde{Q}_7 , so that they do not contribute to the coefficient of the leading dimension-six operator *below* the charm threshold (cf. (1)). Likewise they cannot mix with \tilde{Q}_7 under renormalization.

Therefore our operator basis consists of $Q_{1,2}^{kl}$,

²⁾Here and in the following the superscript “bare” denotes unrenormalized operators, while renormalized ones do not carry an additional superscript.

$Q_{3,\dots,6}$ and \tilde{Q}_7 ³⁾ and $\mathcal{L}_{\text{eff}}^{|\Delta S|=2}$ is found as:

$$\begin{aligned} \mathcal{L}_{\text{eff}}^{|\Delta S|=2} = & -\frac{G_F}{\sqrt{2}} \sum_{i=1}^6 C_i \left[\sum_{j=1}^2 Z_{ij}^{-1} \sum_{k,l=u,c} V_{ks}^* V_{ld} Q_j^{kl,\text{bare}} \right. \\ & \left. - \lambda_t \sum_{j=3}^6 Z_{ij}^{-1} Q_j^{\text{bare}} \right] \\ & - \frac{G_F^2}{2} \lambda_c \lambda_t \left[\sum_{k=1}^2 \sum_{l=1}^6 C_k C_l \tilde{Z}_{kl,7}^{-1} \right. \\ & \left. + \tilde{C}_7 \tilde{Z}_{77}^{-1} \right] \tilde{Q}_7^{\text{bare}} \\ & + \text{counterterms proportional to (12)} \\ & \text{unphysical operators.} \end{aligned}$$

³⁾In addition to these physical operators we have to take into account several evanescent operators. This class of operators appears quite naturally when one has to deal with the renormalization of operators containing more than one fermion line in dimensional regularization [5,8,9]. To illustrate some of the findings of [9] we have defined the evanescent operators with some arbitrary coefficients $a_1, a_2, \tilde{a}_1, \tilde{b}_1$:

$$E_1[Q_j] = \left[\gamma_\mu \gamma_\nu \gamma_\eta L \otimes \gamma^\eta \gamma^\nu \gamma^\mu L \right. \\ \left. - (4 + a_1 \varepsilon) \gamma_\mu L \otimes \gamma^\mu L \right] K_{1j}, \quad j = 1, \dots, 4, \quad (9a)$$

$$E_1[Q_j] = \left[\gamma_\mu \gamma_\nu \gamma_\eta R \otimes \gamma^\eta \gamma^\nu \gamma^\mu L \right. \\ \left. - (16 + a_2 \varepsilon) \gamma_\mu R \otimes \gamma^\mu L \right] K_{1j}, \quad j = 5, 6, \quad (9b)$$

$$E_1[\tilde{Q}_7] = \frac{m_c^2}{g^2} \left[\gamma_\mu \gamma_\nu \gamma_\eta L \otimes \gamma^\eta \gamma^\nu \gamma^\mu L \right. \\ \left. - (4 + \tilde{a}_1 \varepsilon) \gamma_\mu L \otimes \gamma^\mu L \right] K_{12}, \quad (9c)$$

$$E_2[\tilde{Q}_7] = \frac{m_c^2}{g^2} \left[\gamma_\mu \gamma_\nu \gamma_\eta \gamma_\sigma \gamma_\tau L \otimes \gamma^\tau \gamma^\sigma \gamma^\eta \gamma^\nu \gamma^\mu L \right. \\ \left. - [(4 + \tilde{a}_1 \varepsilon)^2 + \tilde{b}_1 \varepsilon] \gamma_\mu L \otimes \gamma^\mu L \right] K_{22}. \quad (9d)$$

with the color factors

$$\begin{aligned} K_{12} = K_{13} = K_{15} &= \frac{1}{2} \tilde{\mathbf{1}} - \frac{1}{2N} \mathbf{1}, \\ K_{11} = K_{14} = K_{16} &= \frac{1}{4} \mathbf{1} + \frac{N^2-2}{4N} \tilde{\mathbf{1}}. \end{aligned} \quad (10)$$

Apart from places where it is indicated we will always state the results corresponding to

$$a_1 = -8, \quad a_2 = -16, \quad \tilde{a}_1 = -8, \quad (11)$$

in order to comply with the standard choice used in [2, 3,5-7]. Since NLO anomalous dimensions and matching corrections of physical operators do not depend on \tilde{b}_1 , we do not give a numerical value. Likewise we do not need the value of the colour factor K_{22} .

2.2. The Effective Lagrangian $\mathcal{L}_{\text{eff}}^{|\Delta S|=2}$ at the Scale μ_{tW}

Besides the operators we need to know their corresponding Wilson coefficient functions at the initial scale μ_{tW} . The ones for the $|\Delta S|=1$ case, C_i , $i = 1, \dots, 6$ can be taken from [5-7]. It is important to note that only C_2 starts at $O(\alpha_s^0)$, the others at $O(\alpha_s^1)$. This means that the NLO matching can be done solely with the diagram D_0 of Fig. 1 with two insertions of Q_2 . One easily finds

$$\tilde{C}_7(\mu_{tW}) = \begin{cases} 0 & \text{in LO} \\ \frac{\alpha_s(\mu_{tW})}{4\pi} \left(-8 \ln \frac{\mu_{tW}}{M_W} \right. \\ \left. + 4F(x_t(\mu_{tW})) + 2 \right) & \text{in NLO} \end{cases}, \quad (13)$$

where $F(x_t)$ is the top dependent part of $S(x_c, x_t)$ defined in (4). The factor α_s originates from the special definition of \tilde{Q}_7 in (7). Note how the large logarithm $\ln x_c$ in (3c) is split between the Wilson coefficient \tilde{C}_7 and the matrix element. The NLO result in (13) is specific to the NDR scheme with (11).⁴⁾

2.3. Evolving down $\mathcal{L}_{\text{eff}}^{|\Delta S|=2}$ from μ_{tW} to μ_c

Next we have to evolve down the Wilson coefficients present in $\mathcal{L}_{\text{eff}}^{|\Delta S|=2}$ (12) from μ_{tW} to μ_c . For the $|\Delta S|=1$ functions C_i , $i = 1, \dots, 6$ this is achieved by standard methods [6]. To calculate the running of the $|\Delta S|=2$ coefficient \tilde{C}_7 we need to derive and solve the corresponding RG equation. From $\mu \frac{d}{d\mu} \mathcal{L}_{\text{eff}}^{|\Delta S|=2} = 0$ in (12) one finds

$$\begin{aligned} \mu \frac{d}{d\mu} \tilde{C}_7(\mu) &= \tilde{C}_7(\mu) \tilde{\gamma}_{77} \\ &+ \sum_{k=1}^2 \sum_{k'=1}^6 C_k(\mu) C_{k'}(\mu) \tilde{\gamma}_{kk',7} \end{aligned} \quad (14)$$

with the *anomalous dimension tensor*⁵⁾

$$\tilde{\gamma}_{kn,7} = \frac{\alpha_s}{4\pi} \tilde{\gamma}_{kn,7}^{(0)} + \left(\frac{\alpha_s}{4\pi} \right)^2 \tilde{\gamma}_{kn,7}^{(1)} + \dots$$

⁴⁾ The Wilson coefficient \tilde{C}_7 depends on \tilde{a}_1 :

$$\tilde{C}_7(\mu_{tW}) = \frac{\alpha_s(\mu_{tW})}{4\pi} \left[-8 \ln \frac{\mu_{tW}}{M_W} + 4F(x_t(\mu_{tW})) - (6 + \tilde{a}_1) \right]$$

⁵⁾ "Anomalous dimension tensor" is clearly a misnomer and only used to distinguish $\tilde{\gamma}_{kn,7}$ from ordinary anomalous dimension (square) matrices.

$$\begin{aligned}
&= - \sum_{k'=1}^2 \sum_{n'=1}^6 [\gamma_{kk'} \delta_{nn'} + \delta_{kk'} \gamma_{nn'}] \tilde{Z}_{k'n',7}^{-1} \tilde{Z}_{77} \\
&\quad - \left[\mu \frac{d}{d\mu} \tilde{Z}_{kn,7}^{-1} \right] \tilde{Z}_{77}. \tag{15}
\end{aligned}$$

It is possible to solve the inhomogeneous equation (14) directly but this turns out to be inconvenient for practical purposes. Instead we may combine the evolution equations of the $|\Delta S|=1$ and $|\Delta S|=2$ Wilson coefficients into a single matrix equation. This is made possible because the GIM mechanism ensures that at least one of the two $|\Delta S|=1$ operator insertions in diagrams like the ones displayed in Fig. 1 is of the current-current type. The current-current part of the $|\Delta S|=1$ mixing matrix, i.e. the entries related to Q_1 , Q_2 , can be diagonalized exactly using the basis

$$Q_{\pm}^{kl} = \frac{1}{2} (Q_2^{kl} \pm Q_1^{kl}). \tag{16}$$

Then (14) together with the RG equation of the $|\Delta S|=1$ Wilson coefficients splits into two independent inhomogeneous RG equations

$$\mu \frac{d}{d\mu} \tilde{C}_7^{\pm}(\mu) = \tilde{\gamma}_{77} \tilde{C}_7^{\pm}(\mu) + \tilde{\gamma}_{\pm k,7} C_{\pm}(\mu) C_k(\mu). \tag{17}$$

Here the decomposition of $\tilde{C}_7(\mu_{tW})$ into $\tilde{C}_7^{\pm}(\mu_{tW})$ is completely arbitrary provided one satisfies

$$\tilde{C}_7(\mu_{tW}) = \tilde{C}_7^+(\mu_{tW}) + \tilde{C}_7^-(\mu_{tW}). \tag{18}$$

This decomposition is then automatically preserved at any renormalization scale.

Each of the two equations in (17) may be written as a 7×7 matrix equation, which may be solved by standard methods. We can even do better and collapse the two resulting 7×7 matrix equations into one 8×8 matrix equation:

$$\mu \frac{d}{d\mu} \vec{D} = \hat{\gamma}^T \cdot \vec{D} \tag{19}$$

with

$$\hat{\gamma}^T = \begin{pmatrix} \gamma^T & 0 & 0 \\ \tilde{\gamma}_{+,7}^T & \tilde{\gamma}_{77} - \gamma_+ & 0 \\ \tilde{\gamma}_{-,7}^T & 0 & \tilde{\gamma}_{77} - \gamma_- \end{pmatrix} \tag{20a}$$

$$\tilde{\gamma}_{\pm,7}^T = (\tilde{\gamma}_{\pm 1,7}, \tilde{\gamma}_{\pm 2,7}, \tilde{\gamma}_{\pm 3,7}, \tilde{\gamma}_{\pm 4,7}, \tilde{\gamma}_{\pm 5,7}, \tilde{\gamma}_{\pm 6,7}) \tag{20b}$$

$$\vec{D}(\mu) = \begin{pmatrix} \vec{C}(\mu) \\ \tilde{C}_7^+(\mu)/C_+(\mu) \\ \tilde{C}_7^-(\mu)/C_-(\mu) \end{pmatrix}. \tag{20c}$$

We now need to know the elements of the anomalous dimension tensor $\tilde{\gamma}_{\pm i,7}$, $i = 1, \dots, 6$. They are obtained from the renormalization constants using the definition in (15) and expanding the quantities in there in powers of α_s and $1/\varepsilon$. Here it is important to include the finite renormalization terms needed for the correct treatment of the evanescent operators (9). To calculate the LO term $\tilde{\gamma}_{\pm i,7}^{(0)}$ one needs to know the $1/\varepsilon$ parts of the one-loop diagrams displayed in Fig. 1, the NLO part $\tilde{\gamma}_{\pm i,7}^{(1)}$ requires the evaluation of a set of two-loop graphs. We find:

$$\tilde{\gamma}_{+,7}^{(0)} = \begin{pmatrix} -16 \\ -8 \\ -32 \\ -16 \\ 32 \\ 16 \end{pmatrix}, \quad \tilde{\gamma}_{-,7}^{(0)} = \begin{pmatrix} 8 \\ 0 \\ 16 \\ 0 \\ -16 \\ 0 \end{pmatrix}, \tag{21a}$$

$$\tilde{\gamma}_{+,7}^{(1)} = \begin{pmatrix} -212 \\ -28 \\ -456 \\ -88 \\ \frac{1064}{3} \\ \frac{832}{3} \end{pmatrix}, \quad \tilde{\gamma}_{-,7}^{(1)} = \begin{pmatrix} 276 \\ -92 \\ 520 \\ -216 \\ -\frac{1288}{3} \\ 0 \end{pmatrix}. \tag{21b}$$

As usual the NLO anomalous dimension tensor depends on the renormalization scheme. The result (21b) corresponds to the NDR scheme with the definition of the evanescent operators corresponding to (11).⁶⁾

3. The NLO calculation of η_3 below the charm threshold

⁶⁾In our two-loop calculation we have kept a_1, a_2, \tilde{a}_1 and \tilde{b}_1 in (9) arbitrary yielding

$$\tilde{\gamma}_{+,7}^{(1)} = \begin{pmatrix} -\frac{188}{3} - \frac{74}{3} a_1 & + \frac{130}{3} \tilde{a}_1 \\ -\frac{100}{3} - \frac{34}{3} a_1 & + \frac{32}{3} \tilde{a}_1 \\ -\frac{1816}{3} - \frac{88}{3} a_1 & + \frac{32}{3} \tilde{a}_1 \\ -\frac{680}{3} - \frac{80}{3} a_1 & + \frac{28}{3} \tilde{a}_1 \\ \frac{1576}{3} + \frac{80}{3} a_1 + \frac{8}{3} a_2 & - \frac{32}{3} \tilde{a}_1 \\ \frac{1664}{3} + \frac{28}{3} a_1 + \frac{52}{3} a_2 & - \frac{28}{3} \tilde{a}_1 \end{pmatrix}, \tag{22a}$$

3.1. The Effective Lagrangian $\mathcal{L}_{\text{eff}}^{|\Delta S|=2}$ at the Scale $\mu_c = O(m_c)$

After integrating out the charm quark all dependence on m_c belongs to the Wilson coefficients. This implies that the term involving \tilde{Q}_7 in (12) has to disappear from the effective lagrangian, because \tilde{Q}_7 contains m_c in its definition (7). Further the $|\Delta S|=1$ operators are neglected in the new effective lagrangian, because the matrix elements of double insertions of these operators are at most proportional to m_s^2 rather than m_c^2 . We have already neglected such terms in all preceding steps.

Therefore the new effective lagrangian to describe the physics below μ_c reads:

$$\mathcal{L}_{\text{eff}}^{|\Delta S|=2} = -\frac{G_F^2}{16\pi^2} \left[\lambda_c^2 \tilde{C}_{S2}^{(c)}(\mu) + \lambda_t^2 \tilde{C}_{S2}^{(t)}(\mu) + \lambda_c \lambda_t \tilde{C}_{S2}^{(ct)}(\mu) \right] \tilde{Z}_{S2}^{-1}(\mu) \tilde{Q}_{S2}^{\text{bare}}. \quad (23)$$

This lagrangian already resembles $-H^{|\Delta S|=2}$ introduced in (1). For the matching we have to set the Green's function derived from (12) and the one derived from (23) equal at the scale $\mu = \mu_c$.

Let us start with the matching of \tilde{C}_7 in the LO: since the definition of \tilde{Q}_7 (7) contains the factor α_s with respect to \tilde{Q}_{S2} we develop an explicit inverse power of α_s for the Wilson coefficient:

$$\tilde{C}_{S2}^{(ct)}(\mu_c) = \frac{m_c^2(\mu_c)}{2} \frac{4\pi}{\alpha_s(\mu_c)} \tilde{C}_7(\mu_c) \text{ in LO} \quad (24)$$

Diagrams containing double insertions are of order α_s^0 and therefore start contributing to $\tilde{C}_{S2}^{(ct)}$ in the NLO. The NLO version of $\tilde{C}_{S2}^{(ct)}$ can be written

$$\begin{aligned} \tilde{C}_{S2}^{(ct)}(\mu_c) &= m_c^2(\mu_c) \left[\frac{1}{2} \frac{4\pi}{\alpha_s(\mu_c)} \tilde{C}_7(\mu_c) \right. \\ &\quad \left. + \sum_{i=+, -} \sum_{j=1}^6 r_{ij, S2}(\mu_c) C_i(\mu_c) C_j(\mu_c) \right] \quad (25) \\ \tilde{\gamma}_{-,7}^{(1)} &= \begin{pmatrix} \frac{124}{3} + \frac{22}{3} a_1 & -\frac{110}{3} \tilde{a}_1 \\ -12 + 6a_1 & +4\tilde{a}_1 \\ \frac{1496}{3} + \frac{8}{3} a_1 & -\frac{16}{3} \tilde{a}_1 \\ -120 + 8a_1 & +4\tilde{a}_1 \\ \frac{1160}{3} - \frac{16}{3} a_1 + \frac{8}{3} a_2 & +\frac{16}{3} \tilde{a}_1 \\ -128 & -4a_1 - 4a_2 & -4\tilde{a}_1 \end{pmatrix} \quad (22b) \end{aligned}$$

The coefficients $r_{ij, S2}(\mu_c)$ in (25) are given by the finite parts of the diagrams in Fig. 1. We find:

$$r_{ij, S2}(\mu_c) = \begin{cases} \left[-4 \ln \frac{m_c(\mu_c)}{\mu_c} - 1 \right] \tau_{ij} & \text{for } j=1, 2, \\ \left[-8 \ln \frac{m_c(\mu_c)}{\mu_c} - 4 \right] \tau_{ij} & \text{for } j=3, 4, \\ \left[8 \ln \frac{m_c(\mu_c)}{\mu_c} + 4 \right] \tau_{ij} & \text{for } j=5, 6, \end{cases} \quad (26)$$

where the τ_{ij} 's denote the colour factors

$$\begin{aligned} \tau_{\pm 1} = \tau_{\pm 3} = \tau_{\pm 5} &= \frac{1 \pm N}{2}, \\ \tau_{+2} = \tau_{+4} = \tau_{+6} &= 1, \\ \tau_{-2} = \tau_{-4} = \tau_{-6} &= 0. \end{aligned} \quad (27)$$

Note that $r_{ij, S2}$ for $j=1, 2$ depends on the definition of the evanescent operator $E_1[\tilde{Q}_7]$. As usual (26) only holds in the NDR scheme.

3.2. Evolving $\mathcal{L}_{\text{eff}}^{|\Delta S|=2}$ below μ_c

The RG running in the effective three quark theory is particularly simple because there is only one operator left: \tilde{Q}_{S2} . The running of the corresponding Wilson coefficient function $\tilde{C}_{S2}^{(ct)}$ can be taken from [5,2].

η_3 can then be determined from the identification

$$\mathcal{L}_{\text{eff}}^{|\Delta S|=2} = -H^{|\Delta S|=2} \quad (28)$$

with $\mathcal{L}_{\text{eff}}^{|\Delta S|=2}$ from (23) and $H^{|\Delta S|=2}$ from (1). The result of this can be found in [4, section 5].

4. Numerical Results

Let us now discuss the numerical implications of the calculation presented in the preceding sections. We will present the dependence of η_3^* on its various physical parameters and on the renormalization scales at which particles are integrated out.

η_3^* depends on the scales μ_{tW} , μ_b and μ_c . Further it is a function of the masses m_t , m_c and of the QCD scale parameter Λ_{QCD} . To establish a starting point let us pick a basic set of input

parameters

$$\begin{aligned}
m_c(m_c) = \mu_c & & \Lambda_{\overline{\text{MS}}} &= 0.31 \text{ GeV}, \\
= 1.3 \text{ GeV}, & & \Lambda_{\text{QCD}}^{\text{LO}} &= 0.15 \text{ GeV}, \\
\mu_b = 4.8 \text{ GeV}, & & M_W &= 80 \text{ GeV}, \\
\mu_{tW} = 130 \text{ GeV}, & & m_t(m_t) &= 167 \text{ GeV}.
\end{aligned}
\tag{29}$$

In the following Λ_{QCD} is always understood to be defined with respect to four active flavours, the corresponding quantities in effective three- and five flavour-theories are obtained by imposing continuity on the coupling α_s at μ_c and μ_b .⁷⁾

The value for η_3^* corresponding to the set (29) reads:

$$\eta_3^{*\text{LO}} = 0.365, \quad \eta_3^{*\text{NLO}} = 0.467.
\tag{30}$$

Hence the NLO calculation has enhanced η_3^* by 27%. From the difference of 0.102 between the two values in (30) 0.022 originates from the change from the LO to the NLO running α_s . The smallness of this contribution is caused by the adjustment of $\Lambda_{\text{QCD}}^{\text{LO}}$ to fit the NLO running coupling. The explicit $O(\alpha_s)$ corrections from the NLO mixing and matching contribute 0.080.

Let us further quantify the influence of the penguin operators $Q_{3,\dots,6}$: If one neglects them completely, one obtains $\eta_3^{*\text{NLO,np}} = 0.472$ with the set in (29), i.e. their contribution is of the order of 1%.

4.1. Scale Dependence of η_3^*

Ideally η_3^* should not depend on the factorization scales μ_{tW} , μ_b , μ_{tW} . Yet due to the truncation of the perturbation series such a dependence shows up. It may serve as an estimate of the theoretical error of the calculation.

It turns out that the dependence of η_3^* on μ_b is extremely mild. This is due to the fact that no diagrams containing internal bottom quarks contribute to the $|\Delta S|=2$ process in order α_s . The only places where μ_b enters are a) the running of α_s , b) the NLO matching matrices and anomalous dimensions of the $|\Delta S|=1$ penguin operators. Numerically one finds that η_3^* is shifted by 0.1–0.2% if one chooses the extreme values of $\mu_b \equiv \mu_c = O(m_c)$ or $\mu_b \equiv \mu_{tW} = O(m_W, m_t)$.

⁷⁾Threshold corrections appearing for $\mu_q \neq m_q$ are numerically negligible.

Now let us turn to the more important cases, μ_{tW} and μ_c . First consider the variation of η_3^* with respect to μ_{tW} , which is displayed in Fig. 2. Since at μ_{tW} the top quark and the W-boson

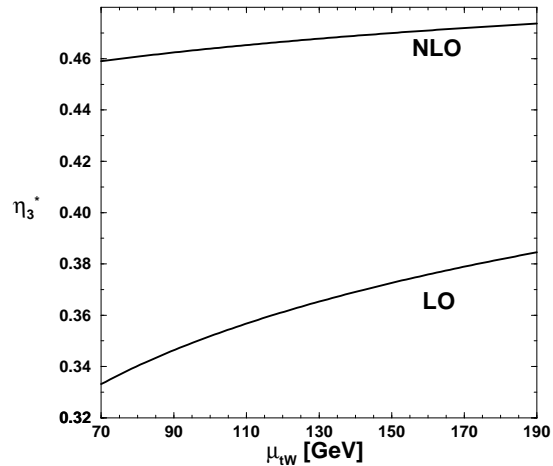


Figure 2. The variation of η_3^* in LO and NLO with respect to the scale μ_{tW} , at which the initial condition is defined. The other input parameters are given in (29).

are integrated out simultaneously, it is natural to choose the interval $M_W \leq \mu_{tW} \leq m_t$ for the analysis. In the LO result for η_3^* we find a sizeable scale dependence of 12%. It is almost totally removed in the NLO, where we obtain a variation of less than 3% in this interval. This shows that it is very accurate to integrate out the two heavy particles simultaneously. The strong improvement in the NLO is due to the smallness of $\ln x_t$.

The situation is not so nice in the case of the variation of μ_c , which is displayed in Fig. 3. We have intentionally extended the range for μ_c to the unphysical low value of 0.7 GeV to visualize the breakdown of perturbation theory. Varying μ_c within the interval $1.1 \text{ GeV} \leq \mu_c \leq 1.6 \text{ GeV}$ yields

$$0.33 \leq \eta_3^{*\text{LO}} \leq 0.40, \quad 0.43 \leq \eta_3^{*\text{NLO}} \leq 0.50.
\tag{31}$$

This corresponds to a reduction of the scale de-

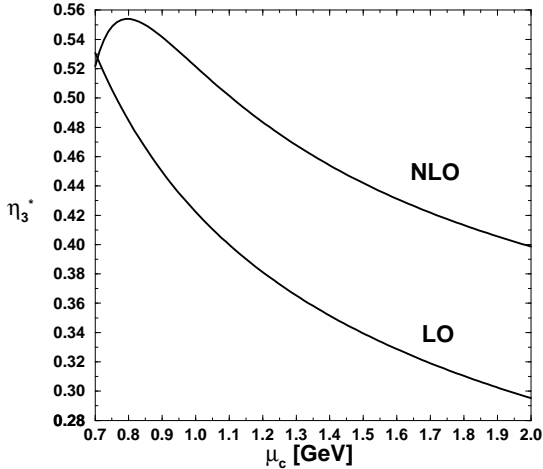


Figure 3. The variation of η_3^* in LO and NLO with respect to the scale μ_c . The range for the latter is taken unphysically large to visualize the breakdown of perturbation theory. The other input parameters are given in (29).

pendence from 20% to 14%. One reason for the poor improvement is the fact that the NLO running of the mass is stronger than the LO one.

4.2. Dependence of η_3^* on Physical Quantities

Let us now investigate the dependence of η_3^* on the physical parameters. From the smallness of the coefficient \tilde{C}_7 at the initial scale one expects η_3^* to be almost independent of $m_t^* = m_t(m_t)$. This statement is confirmed numerically, allowing to treat η_3^* as m_t -independent in phenomenological analyses.

The LO result for η_3^* depends on $m_c^* = m_c(m_c)$ sizeably. Yet this dependence is washed out nearly completely if one looks at the NLO η_3^* , see Fig. 4.

We close this section by a look at the dependence of η_3^* on Λ_{QCD} , which is plotted in Fig. 5. It also turns out to be very moderate.

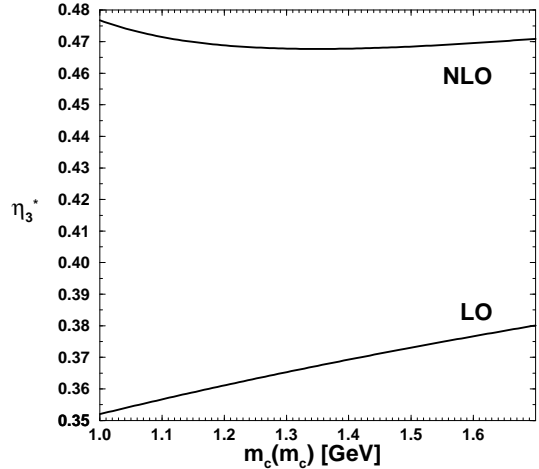


Figure 4. The dependence of η_3^* on $m_c(m_c)$ in LO and NLO. The other input parameters are given in (29).

5. Conclusions

We have calculated the QCD short distance coefficient η_3^* of the low energy $|\Delta S|=2$ hamiltonian in the next-to-leading order (NLO) of renormalization group improved perturbation theory. It reads

$$\eta_3^* = 0.47_{-0.04}^{+0.03}, \quad \eta_3^{*\text{LO}} \approx 0.37. \quad (32)$$

The coefficient is scheme independent except that it depends on the definition of the quark masses in $H^{|\Delta S|=2}$. The result in (32) corresponds to $\overline{\text{MS}}$ -masses $m_c(m_c)$ and $m_t(m_t)$ as indicated by the superscript “*”.

The result has passed several checks:

- i) The NLO anomalous dimension tensor $\tilde{\gamma}_{\pm j,7}$ (21b) has been found independent of the infrared structure of the two-loop diagrams.
- ii) We have kept the gluon gauge parameter ξ arbitrary. It has vanished from $\tilde{\gamma}_{\pm j,7}$ after adding the contributions of the diagrams with their correct combinatorial weight.

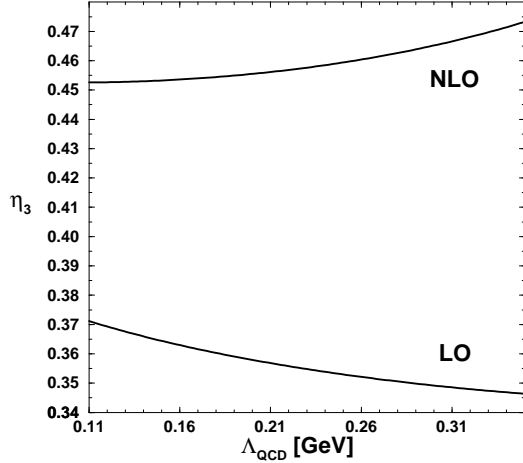


Figure 5. The dependence of η_3^* on Λ_{QCD} in LO and NLO. Actual values for $\alpha_s(M_Z)$ correspond to $\Lambda_{\text{QCD}}^{\text{LO}} \approx 0.15 \text{ GeV}$ and $\Lambda_{\overline{\text{MS}}} \approx 0.31 \text{ GeV}$. The other input parameters are listed in (29).

- iii) $\ln(m_c/\mu)/\varepsilon$ -terms have disappeared from the sum of two-loop diagrams and counterterm diagrams.
- iv) The dependences of the final result for η_3^* on the matching scales μ_{tW} , μ_b and μ_c cancel to order α_s . Numerically the dependence has decreased.
- v) If one expands the final result in powers of α_s , one recovers the terms proportional to $\alpha_s^0 \ln^1 x_c$, $\alpha_s^0 \ln^0 x_c$, $\alpha_s^1 \ln^2 x_c$, $\alpha_s^1 \ln^1 x_c$ of the result without RG improvement.
- vi) The initial condition for \tilde{C}_7 in (13) as well as the anomalous dimension tensor $\tilde{\gamma}_{\pm j,7}$ in (21b) depend on the definition of the evanescent operators (9). We have checked that this dependence is in accordance with the theorems of [9], so that the final result is independent of the choice of the evanescent operators.

REFERENCES

1. F. J. Gilman and M. B. Wise, Phys. Rev. D27 (1983) 1128.
2. A. J. Buras, M. Jamin and P. H. Weisz, Nucl. Phys. B347 (1990) 491.
3. S. Herrlich and U. Nierste, Nucl. Phys. B419 (1994) 292.
4. S. Herrlich and U. Nierste, *The Complete $|\Delta S|=2$ -Hamiltonian in the Next-To-Leading Order*, preprint **hep-ph/9604330**, DESY 96-048, TUM-T31-86/96.
5. A. J. Buras and P. H. Weisz, Nucl. Phys. B333(1990)66.
6. A. J. Buras, M. Jamin, M. E. Lautenbacher and P. H. Weisz, Nucl. Phys. B370 (1992) 69, addendum Nucl. Phys. B375 (1992) 501.
7. A. J. Buras, M. Jamin, M. E. Lautenbacher and P. H. Weisz, Nucl. Phys. B400 (1993) 37-74.
8. M. J. Dugan and B. Grinstein, Phys. Lett. B256 (1991) 239.
9. S. Herrlich and U. Nierste, Nucl. Phys. B455 (1995) 39-58.